

# Catalytic wet peroxide oxidation for organic wastewater treatment by $\text{Fe}_2\text{O}_3/\text{Al}_2\text{O}_3$ catalyst coupled with membrane

LIU Yiwei, QUAN Xie\*, CHEN Shuo, YU Hongtao, DU Lei

( Key Laboratory of Industrial Ecology and Environmental Engineering, Ministry of Education,  
Dalian University of Technology, Dalian 116024, China )

**Abstract:** A reactor coupling catalytic wet peroxide oxidation (CWPO) with ceramic tubular membrane separation was designed for efficiency improvement of degradation of organic wastewater. The membrane was fabricated by coating  $\text{Fe}_2\text{O}_3/\text{Al}_2\text{O}_3$  on the membrane support by the sol-gel method. The pore size of prepared membrane was optimized to the range of ultrafiltration by controlling PVA concentration and coating times. The CWPO experiment was conducted in various operating conditions to select the optimal pH, working temperature, pressure and  $\text{H}_2\text{O}_2$  concentration. The phenol degradation results show complete phenol degradation and 70% TOC removal within 150 min under pH 6, 90 °C, 0.4 MPa when the  $\text{H}_2\text{O}_2$  concentration is 20 mmol/L. The results of five consecutive and dissolution experiments illustrate good stability and repeatability of the  $\text{Fe}_2\text{O}_3/\text{Al}_2\text{O}_3$  ceramic membrane. The reactor coupling CWPO with membrane separation presents new insights into the field of organic wastewater treatment.

**Key words:** catalytic wet peroxide oxidation;  $\text{Fe}_2\text{O}_3/\text{Al}_2\text{O}_3$  membrane catalyst; phenol; advanced oxidation technologies (AOTs)

## 0 Introduction

Advanced oxidation technologies (AOTs), such as catalytic ozonation, Fenton-like reaction, photo-catalysis and catalytic wet peroxide oxidation (CWPO), which are based on the generation of reactive oxygen species (ROS) for refractory organic pollutants degradation, are efficient processes for water treatment<sup>[1-2]</sup>. Amongst these AOTs, catalytic wet peroxide oxidation, in which  $\text{H}_2\text{O}_2$  is catalyzed by various catalysts to generate hydroxyl radicals ( $\cdot\text{OH}$ ), has attracted increasing attention for the degradation

of refractory organic pollutants in water<sup>[3-4]</sup>.

The catalysts applied in the CWPO process are mostly heterogeneous catalysts rather than homogeneous catalysts because homogeneous catalysts usually suffer from secondary pollution and the difficulties in recycle and reuse<sup>[5]</sup>. However, the catalytic performance of heterogeneous catalysts is generally far away from that of homogeneous catalysts due to the poor mass transfer process. To enhance the catalytic performance of heterogeneous catalysts towards CWPO, a quest is initiated to construct

Received by: 2019-05-20; Revised by: 2019-10-10.

Supported by: National Natural Science Foundation of China (Major Project; No. 21590813); Liaoning Revitalization Talents Program(XLYC1801003).

Corresponding authors: LIU Yiwei(1994-), Female, Master, E-mail:2012liuyiwei@mail.dlut.edu.cn; QUAN Xie\* (1960-), Male, Prof., E-mail:quanxie@dlut.edu.cn.

a system that could improve the mass transfer process.

Membrane reactor is a flow-through system in which chemical reaction and membrane separation are coupled in one unit. The membrane with porous structure could act as the catalyst carrier<sup>[6]</sup>. The porous structure of membrane could decrease the diffusion resistance for mass transfer, which favors the efficient transfer of reactants to the active components. Moreover, conducting CWPO in micro or nanostructures could further optimize the availability of active sites because of the nanoscale effect<sup>[7]</sup>. Therefore, it could be speculated that coupling CWPO with membrane separation processes could enhance the catalytic performance for organic pollutant degradation.

In this work, to improve the mass transfer process and enhance the catalytic performance of CWPO process, a coupled CWPO/membrane system was constructed by using a tubular ceramic membrane as the membrane and  $\text{Al}_2\text{O}_3/\text{Fe}_2\text{O}_3$  as a heterogeneous catalyst. The ceramic membrane supported  $\text{Fe}_2\text{O}_3$  was prepared by a dip-coating and calcination method. The pore size of the membrane was controlled by changing the coating times and PVA concentration. The membrane was characterized by scanning electronic microscopy (SEM), X-ray photoelectron spectra (XPS), X-ray diffraction (XRD), thermo gravimetric analysis (TG) and pore size distribution. Phenol was selected as a model organic pollutant. And the catalytic performance was evaluated in a flow membrane reactor at low temperature (60–100 °C) and low pressure (0.2–0.5 MPa). Moreover, a possible catalytic mechanism was also proposed.

## 1 Experimental

### 1.1 Materials

The pristine tubular ceramic membrane (80 mm in length, 12 mm outer diameter, 8 mm inner diameter, 400 nm pore size) was purchased from Jiexi Lishun Technology Co., Ltd.

Polyvinyl alcohol (PVA,  $\geq 99.0\%$ ) was acquired from Sinopharm Chemical Reagent Co., Ltd. (China).  $\text{FeCl}_3 \cdot 6\text{H}_2\text{O}$  ( $\geq 99.0\%$ ), phenol, ammonium hydroxide (25%–28%) and  $\text{AlCl}_3 \cdot 6\text{H}_2\text{O}$  ( $\geq 97.0\%$ ) were purchased from the Damao Chemical Reagent Factory Co., Ltd. (China).  $\text{H}_2\text{O}_2$  (30%) was purchased from the Bo Di Chemical Co., Ltd. (Tianjin, China). All of the materials which be used as received without further purification were analytical grade. Ultrapure water (18.2 M $\Omega$  · cm) was used in all experimental process.

### 1.2 Preparation of $\text{Fe}_2\text{O}_3/\text{Al}_2\text{O}_3$ catalytic membrane

The  $\text{Fe}_2\text{O}_3/\text{Al}_2\text{O}_3$  catalytic membrane was prepared by using a dip-coating and calcination method<sup>[8]</sup>.

Firstly, the sols of  $\text{Fe}(\text{OH})_3$  and  $\text{Al}(\text{OH})_3$ -PVA were prepared. For preparing  $\text{Fe}(\text{OH})_3$  sol, 25 mL  $\text{FeCl}_3$  solution (1 g/L) was added into 75 mL boiling water with continuous stirring for 2 h. For preparing  $\text{Al}(\text{OH})_3$ -PVA sol, 35 mL ammonia hydroxide (5.0 mol/L) was drop-wise added into a 65 mL solution containing 14.9 g  $\text{AlCl}_3 \cdot 6\text{H}_2\text{O}$  under continuous stirring until forming a clear solution, then 3 g PVA particles (soaked in ultrapure water for 12 h before using) were added into the solution. The suspension was kept stirring at 90 °C until PVA particles dissolved completely. The  $\text{Fe}(\text{OH})_3$ - $\text{Al}(\text{OH})_3$ -PVA sol-gel was prepared by mixing the  $\text{Fe}(\text{OH})_3$  sol and the  $\text{Al}(\text{OH})_3$ -PVA sol (1 : 1, V/V). To investigate the influence of PVA concentration,  $\text{Al}(\text{OH})_3$ -PVA sol with 5 g PVA was also prepared with the same procedure and used for preparing the  $\text{Fe}(\text{OH})_3$ - $\text{Al}(\text{OH})_3$ -PVA sol-gel.

For the dip-coating process, the pristine tubular ceramic membranes were immersed vertically into the sol for 2 min. The dip-coating descent and ascent rate was 1 000  $\mu\text{m/s}$  and 100  $\mu\text{m/s}$ , respectively. Then the membrane was dried in oven for 6 h at 80 °C. Finally, to remove the PVA, the coated membrane was calcined at 550 °C in a muffle furnace for 1 h

with  $1\text{ }^\circ\text{C} \cdot \text{min}^{-1}$  heating rate.

### 1.3 Characterization

The surface morphology of the prepared catalyst was examined by a Hitachi S-4800 scanning electron microscope (SEM, Japan). The relevant parameters of the SEM were set to:  $5\text{ }\mu\text{A}$  current,  $5\text{ kV}$  acceleration voltage,  $8.0\text{ mm}$  working distance. TG-DTG 6300 thermogravimetric analyzer (Japan) was used to study the calcinations process of  $\text{Fe}(\text{OH})_3\text{-Al}(\text{OH})_3\text{-PVA}$  sol-gel with  $5\text{ }^\circ\text{C} \cdot \text{min}^{-1}$  heating rate from room temperature to  $700\text{ }^\circ\text{C}$  at air flow of  $60\text{ mL} \cdot \text{min}^{-1}$ .  $\text{Fe}_2\text{O}_3\text{-Al}_2\text{O}_3$  powder prepared in the same method without coating on ceramic membrane was used for crystallographic structure characterization, and the sample was tested by X-ray diffraction (XRD) on an Emyprean diffractometer by  $\text{CuK}\alpha$  radiation ( $\lambda = 0.154\text{ 056 nm}$ ) when the  $2\theta$  range is from  $5^\circ$  to  $90^\circ$ . X-ray photoelectron spectra (XPS) was measured by Escalab 250 Xi spectrometer ( $\text{AlK}\alpha$  X-ray source, Thermo Fisher Scientific, USA) to investigate the elements composition and valence state.

The pore size distribution of the catalytic membrane was measured by Porolux 1000 membrane pore size distribution tester (IB-FT GmbH, Germany) with the pressure range from 0 to  $1.5\text{ MPa}$ . Pure water flux ( $J$ ) was determined by membrane filtration (dead end) experiments and the results were calculated as follows:

$$J = V/Stp \quad (1)$$

Where  $V(\text{L})$  is the filtered water's volume,  $t(\text{h})$  is the actual permeating time,  $S(\text{m}^2)$  is the effective membrane area,  $p(0.1\text{ MPa})$  is the pressure difference of the membrane.

Phenol degradation performance was detected by high performance liquid chromatography (Waters, 1200) at  $271\text{ nm}$  using a UV detector (Waters, 2695) with a C18 column. A mixture of water and methanol ( $30 : 70, V/V$ ) was used to be the mobile phase, and the column temperature was set at  $30\text{ }^\circ\text{C}$ . The total organic carbon (TOC) concentration was determined by

multi N/C 2100S tester (Germany, Analytikjena). The concentration of dissolved Fe ions in effluent was analyzed by inductively coupled plasma optical emission spectrometry (ICP, USA). The reactive oxidative species were investigated by electron paramagnetic resonance (EPR) at the condition of  $9.5\text{ GHz}$  microwave frequency and  $0.336\text{ T}$  central magnetic field.  $20\text{ }\mu\text{L}$   $0.05\text{ mmol/L}$  DMPO was mixed with  $0.5\text{ mL}$  sample for each test.

### 1.4 Catalytic activity tests and analysis

The catalytic performance of  $\text{Fe}_2\text{O}_3/\text{Al}_2\text{O}_3$  catalytic membrane was operated in a dead-end stainless steel reactor with actual volume about  $2\text{ L}$  as shown in Fig. 1.  $100 \times 10^{-6}$  phenol and different amount of  $\text{H}_2\text{O}_2$  were added into the reactor in sequence. The initial pH was tuned with  $\text{H}_2\text{SO}_4(0.1\text{ mol/L})$  and  $\text{NaOH}(0.1\text{ mol/L})$ . Reactor was kept at constant temperature by using a heating jacket. And the working pressure was supplied by a nitrogen gas cylinder.  $0.05\text{ mL}$   $\text{Na}_2\text{S}_2\text{O}_3(0.1\text{ mol/L})$  was immediately added to the  $1\text{ mL}$  effluent for quenching the residual  $\cdot\text{OH}$  before test. The control experiments were measured at the same reaction condition sampling from the cross-flow model without permeating through the membrane. In the reusability experiment, the  $\text{Fe}_2\text{O}_3/\text{Al}_2\text{O}_3$  membrane was washed with water and dried at  $100\text{ }^\circ\text{C}$ , and then reused in a new reaction.

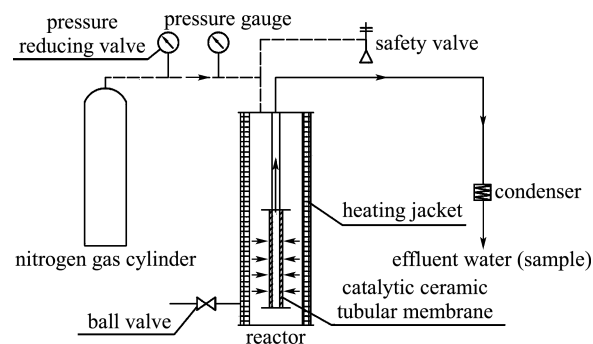


Fig. 1 Diagram of the CWPO reaction system

## 2 Results and discussion

### 2.1 Characterizations of $\text{Fe}_2\text{O}_3/\text{Al}_2\text{O}_3$ membrane

The morphologies of  $\text{Fe}_2\text{O}_3/\text{Al}_2\text{O}_3$  catalytic

membrane and pristine membrane were characterized by SEM on surface and section presented in Fig. 2 at the same amplification factors. Compared with pristine membrane in Fig. 2(a), the surface of  $\text{Fe}_2\text{O}_3/\text{Al}_2\text{O}_3$  catalytic membrane (Fig. 2(d)) is quite flat without any crack, which means that the functional layer is smooth and catalyst particles are distributed evenly. As seen in Fig. 2(b), (e), the diameter of particles in  $\text{Fe}_2\text{O}_3/\text{Al}_2\text{O}_3$  catalytic membrane is smaller than that of particles in pristine

membrane. And  $\text{Fe}_2\text{O}_3/\text{Al}_2\text{O}_3$  catalyst particles are 20-50 nm for the agglomeration phenomenon and distributed equally in the functional layer.

From the cross-section view in Fig. 2(f), the coated catalyst was impregnated into the ceramic membrane substrate with a thickness of 4-5  $\mu\text{m}$  which was thicker than 1  $\mu\text{m}$  of the pristine functional layer. Therefore, the sol-gel method with facile membrane-forming PVA<sup>[9]</sup> immobilized the catalyst and a uniform membrane surface was prepared.

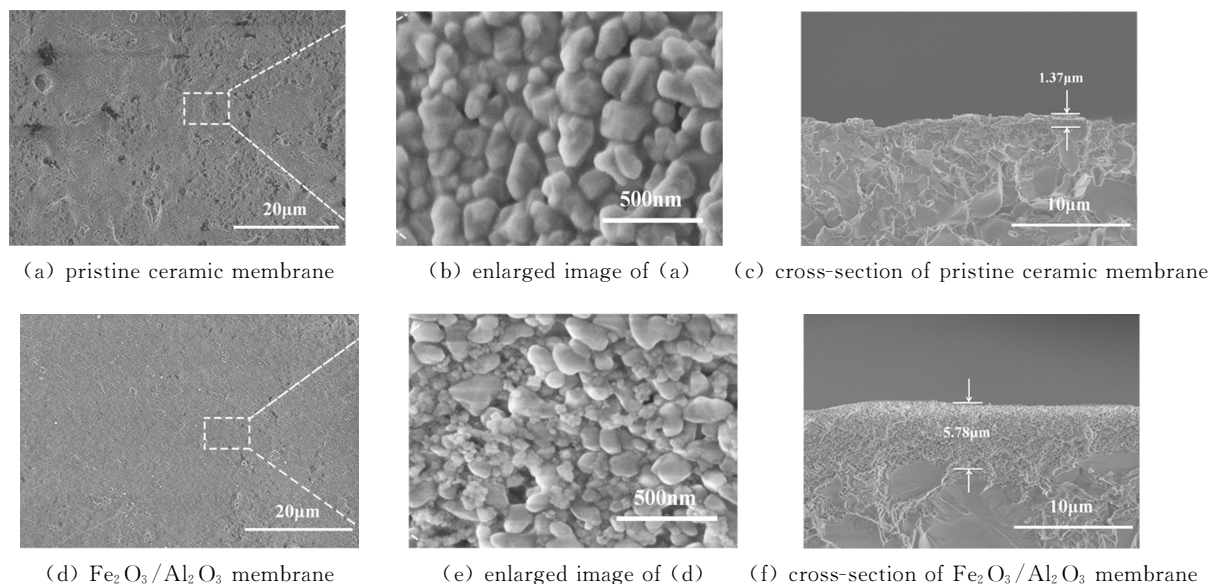


Fig. 2 SEM images

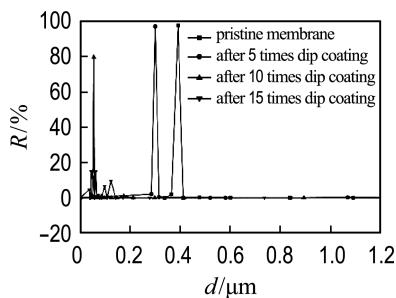
During the preparation process, the concentration of PVA affects the thickness of the functional layer and the pore size of the membrane. Thus, the relationship between pore size of the membrane and coating times of  $\text{Fe}(\text{OH})_3\text{-Al}(\text{OH})_3\text{-PVA}$  (PVA 3%, 5%) sol was investigated and the data were presented in Tab. 1. Fig. 3(a) shows the pore size of the 3%-PVA membrane marked decreases with the coating times increasing. For example, the pore size is 300.0 nm after 5 times of coating while the pore size reduces to 47.6 nm after 15 times of coating. And Fig. 3(b) presents the pore size of the 5%-PVA membrane with 251.8, 137.8 and 115.9 nm after 5, 7, 10 coating times (more coating times brought crack on surface). Thus,

Tab. 1 Pore size and flux of 3%/5%-PVA  $\text{Fe}_2\text{O}_3/\text{Al}_2\text{O}_3$  membrane with different coating times

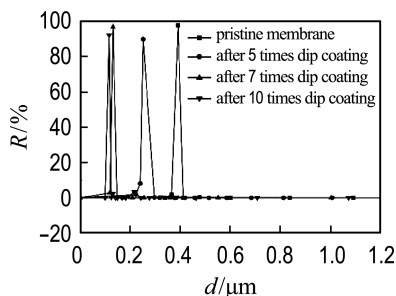
$\omega(\text{PVA})/\%$	times	MFP/ nm	flux/ ( $10 \text{ L} \cdot \text{m}^{-2} \cdot \text{h}^{-1} \cdot \text{MPa}^{-1}$ )
3	pristine	400.8	637.12
	5	300.0	58.94
	10	54.6	34.30
	15	47.6	$\approx 0$
5	pristine	400.8	637.12
	5	251.8	34.30
	7	137.8	18.65
	10	115.9	11.77

the pore size of 3%-PVA membrane decreases much faster with stable and smooth surface. The reason is that high PVA concentration would increase the viscosity of sol-gel and lead a thicker

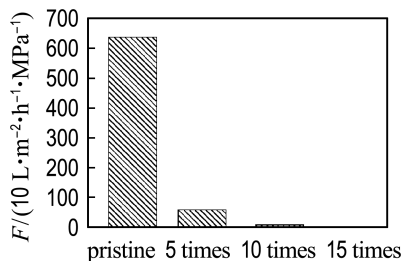
functional layer after dipped. And thicker functional layer is easier to crack than thin one during the calcination process which may be due to the influence of thermal conductivity<sup>[10]</sup>. Therefore, the optimum PVA concentration of  $\text{Fe}(\text{OH})_3\text{-Al}(\text{OH})_3\text{-PVA}$  sol-gel is 3%.



(a) 3% PVA



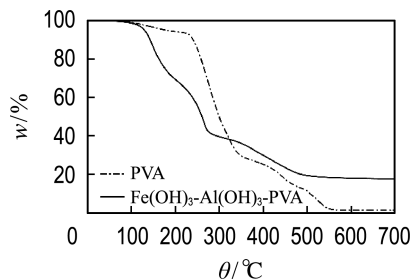
(b) 5% PVA

(c) flux of  $\text{Fe}_2\text{O}_3/\text{Al}_2\text{O}_3$  membrane coated by 3% PVA with different timesFig. 3 Pore size distribution of  $\text{Fe}_2\text{O}_3/\text{Al}_2\text{O}_3$  membrane

Tab. 1 also shows the pure water flux of these 3%-PVA membranes with 5, 10 and 15 coating times. The pore size and the flux gradually decrease as the coating times increases. The flux significantly drops to  $343 \text{ L} \cdot \text{m}^{-2} \cdot \text{h}^{-1} \cdot \text{MPa}^{-1}$  after 10 coating times. And the flux is little at 15 coating times at 0.1 MPa test pressure. Therefore, the 3%-PVA membranes with 10 coating times are used to be the catalytic wet oxidation catalysts ultrafiltration membranes

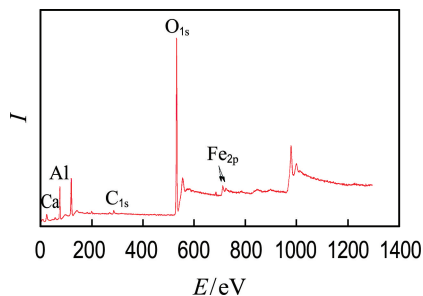
with an eye of pore size and flux.

Thermo gravimetric analysis is an effective measure to analyze the calcination process. As illustrated in Fig. 4, the curves of PVA and  $\text{Fe}(\text{OH})_3\text{-Al}(\text{OH})_3\text{-PVA}$  exist a similar tendency and keep constant after complete decomposition of PVA at  $550^\circ\text{C}$ . Compared with the PVA decomposition, the first rapid weight loss of  $\text{Fe}(\text{OH})_3\text{-Al}(\text{OH})_3\text{-PVA}$  from  $110^\circ\text{C}$  to  $180^\circ\text{C}$  is due to the evaporation of absorbed water in sol-gel. The second fast declined process of prepared sol-gel from  $235^\circ\text{C}$  to  $275^\circ\text{C}$  mostly belongs to the decomposition of PVA. Weight loss from  $275^\circ\text{C}$  to  $500^\circ\text{C}$  is due to the oxidation of  $\text{Fe}(\text{OH})_3\text{-Al}(\text{OH})_3$  sol-gel and further decomposition of PVA, while the thermal stability of PVA may be affected by the existence of aluminum and iron oxides<sup>[8]</sup>. Little weight loss is observed for the sol-gel after  $500^\circ\text{C}$  which indicates the sol-gel has been transformed to target catalyst completely. To avoid residual PVA,  $550^\circ\text{C}$  is chosen for catalyst preparation in the following experiment.

Fig. 4 Thermo gravimetric analysis of  $\text{Fe}(\text{OH})_3\text{-Al}(\text{OH})_3\text{-PVA}$  sol-gel

The XPS spectra of the prepared sample are shown in Fig. 5. Fig. 5(a) is a full spectrum of the catalyst which means the existence of Al, Fe and O elements. The diffraction peaks between 710 eV and 725 eV are attributed to the  $\text{Fe}_{2p}$  diffraction peak and its high-resolution map is presented in Fig. 5(b). It can be seen that 710.9 eV and 724.6 eV correspond to  $\text{Fe}_{2p_{3/2}}^{2+}$  peak and  $\text{Fe}_{2p_{1/2}}^{2+}$  peak, 712.3 eV and 726.4 eV correspond to  $\text{Fe}_{2p_{3/2}}^{3+}$  peak and  $\text{Fe}_{2p_{1/2}}^{3+}$  peak respectively. Furthermore, the peak at 719.2 eV is the

satellite peak of  $\text{Fe}_{2p_{3/2}}^{3+}$ , and 714.7 eV and 733.5 eV correspond to  $\text{Fe}_{\text{sat} 2p_{3/2}}^{2+}$  and  $\text{Fe}_{\text{sat} 2p_{1/2}}^{3+}$  separately. In all, the compositions of iron which load on membrane are mainly  $\text{FeO}$  and  $\text{Fe}_2\text{O}_3$ .



(a) full spectrum

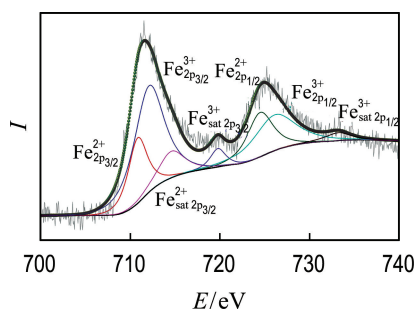
(b)  $\text{Fe}_{2p}$  spectra of  $\text{Fe}_2\text{O}_3/\text{Al}_2\text{O}_3$  catalyst

Fig. 5 XPS spectra

The crystal structure of the prepared catalyst was characterized by XRD, and the results are shown in Fig. 6. Through phase analysis, combined with a standard XRD card (JCPDS card No. 50-0741), the calcined alumina exhibits characteristic peaks (311), (400) and (440) of  $\gamma\text{-Al}_2\text{O}_3$  at  $37.54^\circ$ ,  $45.67^\circ$  and  $66.60^\circ$  which demonstrate the presence of  $\gamma\text{-Al}_2\text{O}_3$ . Comparing to the standard card (JCPDS card No. 33-0664), characteristic peaks (104),

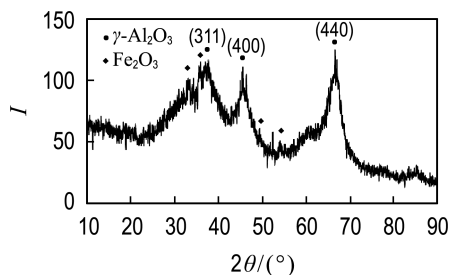
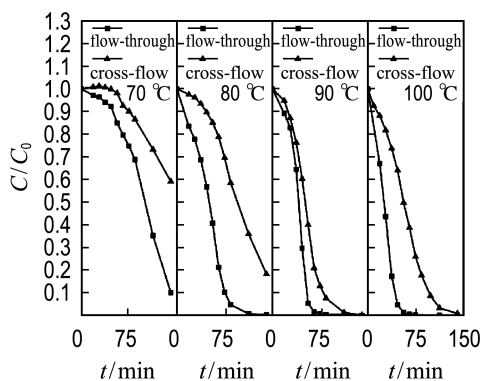


Fig. 6 XRD analysis of catalyst

(110), (024) and (116) indicate the presence of iron oxide. However, these peaks of iron oxide are not obvious for the reason that alumina is relatively large and covers iron oxide.

## 2.2 Catalytic performance of $\text{Fe}_2\text{O}_3/\text{Al}_2\text{O}_3$ membrane

Control experiments were conducted to compare the phenol removal efficiency of cross-flow model with flow-through model. The cross-flow model control experiments simulate a fixed bed that the mass transfer only occurs on the surface of catalyst. As seen in Fig. 7, a better degradation efficiency is obtained in flow-through model than that in cross-flow model. This might be related to better mass transfer in flow-through model. Therefore, it could be concluded that the flow-through  $\text{Fe}_2\text{O}_3/\text{Al}_2\text{O}_3$  membrane coupling CWPO is beneficial to improve degradation efficiency.

Fig. 7 Control experiments on phenol degradation rate (10 mmol/L  $\text{H}_2\text{O}_2$ , 0.3 MPa, pH 6)

The home-made catalytic wet peroxide oxidation membrane reactor was adopted in this study, and phenol was selected as the target contaminant. The initial mass fraction of phenol was  $100 \times 10^{-6}$ . Experiments were conducted at different pH, temperatures, pressures and the concentrations of  $\text{H}_2\text{O}_2$  to seek for an optimal reaction condition.

The effect of pH was investigated primarily with 10 mmol/L  $\text{H}_2\text{O}_2$  under 0.3 MPa,  $90^\circ\text{C}$ . As illustrated in Fig. 8, the concentration of phenol decreases with time in all cases. And the highest reaction efficiency is obtained in initial

phenol solution ( $\text{pH} = 6$ ) with 95% phenol removal rate within 60 min. Moreover, phenol removal rate decreases with the dropping pH from 6 to 3, which is different to the performance of  $\text{Fe}_2\text{O}_3/\text{Al}_2\text{O}_3$  particles catalyst reported previously<sup>[11]</sup>. This unusual result may be due to the flow-through model which causes iron ions to pass through the membrane without being involved in the reaction, as can be known that increasing acidity of the solution leads to more dissolution of the metal ion. When those active iron ions leach and drain with flow, the phenol removal rate decreases. Taking the removal efficiency and stability into consideration, pH 6 is operated in the following experiment.

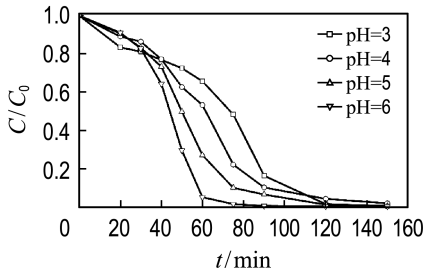


Fig. 8 Effect of initial pH on phenol degradation rate (10 mmol/L  $\text{H}_2\text{O}_2$ , 0.3 MPa, 90 °C)

The oxidation of phenol on the catalytic wet peroxide oxidation membrane at different temperatures was investigated, and the results are presented in Fig. 9. It can be seen that the temperature has a significant effect on the degradation efficiency of phenol. For example, 95% degradation efficiency is got at 100 °C in 50 min, which is much larger than the 8%

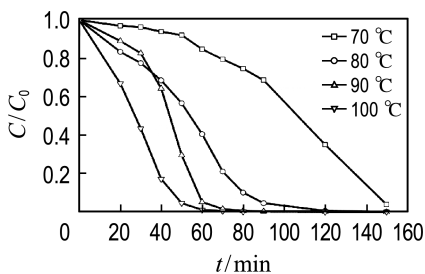


Fig. 9 Effect of working temperature on phenol degradation rate (10 mmol/L  $\text{H}_2\text{O}_2$ , 0.3 MPa, pH 6)

degradation efficiency at 70 °C. Moreover, nearly 100% degradation efficiency is attained at 90 °C after 60 min, which is comparable with it at 100 °C. It is energy-saving that the reaction temperature is selected at 90 °C.

The working pressure is a crucial parameter in this system, as it has a significant impact on the flow rate that liquid permeates through the catalytic membrane and reaction rate. The results of phenol degradation performed under different pressures at 90 °C are shown in Fig. 10. It could be seen that the degradation efficiency under 0.5 MPa pressure is the lowest. This is attributed to that the flow-through rate is quicker than the reaction rate, so the oxidation can't react completely. The degradation efficiency of phenol at 0.2 MPa is less than the ones at 0.3 and 0.4 MPa due to low reaction rate under 0.2 MPa. However, high pressure brings high flow rate (Tab. 2) and reaction rate, and low pressure leads to low flow rate and reaction rate. The results under 0.3 and 0.4 MPa both show a better phenol degradation performance than 0.2 MPa, since a trade-off is set up between flow rate and reaction rate. The flow rate at 0.4 MPa is 2.4 times of that at 0.3 MPa when the degradation efficiency is similar. In consideration

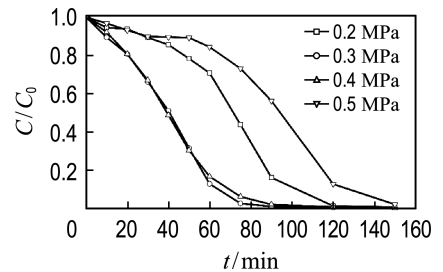


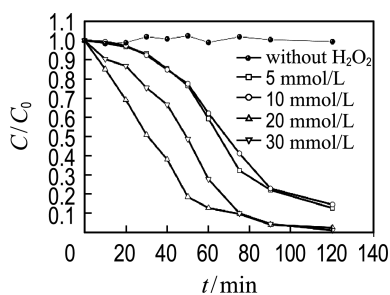
Fig. 10 Effect of working pressure on phenol degradation rate (10 mmol/L  $\text{H}_2\text{O}_2$ , 90 °C, pH 6)

Tab. 2 Flow rate at different working pressures

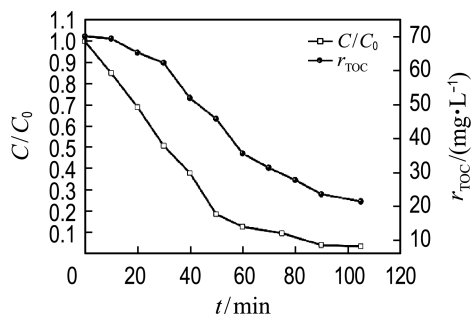
working pressure/MPa	flow rate/(mL · min <sup>-1</sup> )
0.2	0.45
0.3	1.09
0.4	2.61
0.5	3.45

of water treatment performance and economical efficiency, 0.4 MPa is chosen as the optimized working pressure.

Initial concentration of the  $\text{H}_2\text{O}_2$  is also an important factor for the removal efficiency during CWPO process. The results show nearly no phenol degradation is observed on the  $\text{Fe}_2\text{O}_3/\text{Al}_2\text{O}_3$  catalytic membrane with the absence of  $\text{H}_2\text{O}_2$  (Fig. 11(a)). The degradation efficiency increases from 5 mmol/L  $\text{H}_2\text{O}_2$  to 20 mmol/L  $\text{H}_2\text{O}_2$  for the reason that higher concentration  $\text{H}_2\text{O}_2$  generates more oxidizing  $\cdot\text{OH}$  to enhance the phenol removal. However, compared with that of 20 mmol/L  $\text{H}_2\text{O}_2$ , the removal efficiency at 30 mmol/L  $\text{H}_2\text{O}_2$  reduces. The reason is that excess  $\text{H}_2\text{O}_2$  suppresses the generation of  $\cdot\text{OH}$  and forms less reactive species such as hydroperoxyl radicals, which could be hard to participate in the reaction<sup>[12]</sup>.



(a) Effect of  $\text{H}_2\text{O}_2$  concentration on phenol degradation rate (0.4 MPa, 90 °C, pH 6)



(b) Phenol degradation and TOC removal rate (20 mmol/L  $\text{H}_2\text{O}_2$ , 0.4 MPa, 90 °C, pH 6)

Fig. 11 Phenol degradation and TOC removal rate under different conditions

At the optimized conditions, the TOC conversion is 70%, the concentration of TOC decreases from 70.23 mg/L to 21.52 mg/L

(Fig. 11(b)), which means a fast rate of mineralization but still has some residual by-products, such as acetic acid, oxalic acid, hydroquinone and catechol<sup>[13]</sup>.

### 2.3 Stability and reusability of $\text{Fe}_2\text{O}_3/\text{Al}_2\text{O}_3$ membrane

The iron leaching concentration is an indicator to evaluate the stability and environmental security of catalyst. As shown in Fig. 12, about 0.4 mg/L iron leaches into effluent in 150 min (pH 6, 90 °C, 0.4 MPa, 20 mmol/L  $\text{H}_2\text{O}_2$ ), which is far less than 2 mg/L (the environmental standard imposed by the European Union). In the mass, the negligible leaching of iron suggests that the  $\text{Fe}_2\text{O}_3/\text{Al}_2\text{O}_3$  membrane is stable enough to work as a heterogeneous catalytic membrane in CWPO process.

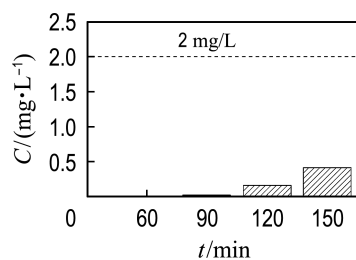


Fig. 12 Iron leaching concentration with reaction time (20 mmol/L  $\text{H}_2\text{O}_2$ , 0.4 MPa, 90 °C, pH 6)

The stability and reusability of the catalyst are also important indicators for the performance of the catalyst, except for the catalytic activity. As shown in Fig. 13, in five consecutive experiments, the removal rates of phenol are 98%, 99%, 97%, 95%, 94% respectively which indicate the good stability of  $\text{Fe}_2\text{O}_3/\text{Al}_2\text{O}_3$  membrane in the CWPO process. The good recyclability ensures the service life of the membrane which means a better application prospect.

### 2.4 Reactive oxidative species and mechanism discussion

The reactive oxidative species generated in  $\text{Fe}_2\text{O}_3/\text{Al}_2\text{O}_3$  membrane catalyzed CWPO process were detected by using electron paramagnetic resonance (EPR) measurement with DMPO as a trapping agent. As shown in Fig. 14, no

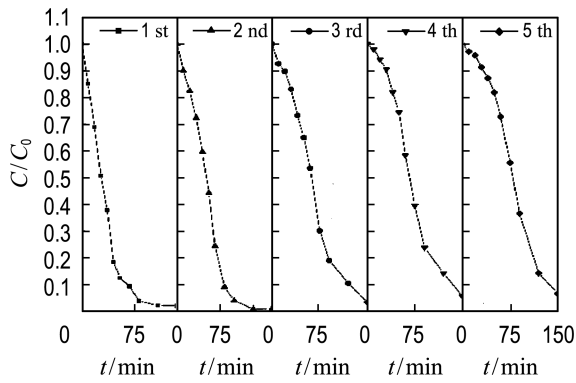


Fig. 13 Reusability of  $\text{Fe}_2\text{O}_3/\text{Al}_2\text{O}_3$  membrane on phenol degradation (20 mmol/L  $\text{H}_2\text{O}_2$ , 0.4 MPa, 90 °C, pH 6)

characteristic peaks are observed with  $\text{H}_2\text{O}_2$  alone. However, once the  $\text{Fe}_2\text{O}_3/\text{Al}_2\text{O}_3$  membrane is added, four characteristic peaks with an intensity ratio of 1 : 2 : 2 : 1 which correspond to  $\text{DMPO} \cdot \text{OH}$  adduct are observed<sup>[14]</sup>. This result indicates that  $\cdot\text{OH}$  is the main reactive oxidative species generated in  $\text{Fe}_2\text{O}_3/\text{Al}_2\text{O}_3$  membrane catalytic reaction. For the  $\text{Fe}_2\text{O}_3/\text{Al}_2\text{O}_3$  membrane catalytic system, the catalytic mechanism is similar with Fenton-like reaction. In light of the experimental results in this paper and previous literatures<sup>[15-16]</sup>, the following catalytic mechanism is proposed.

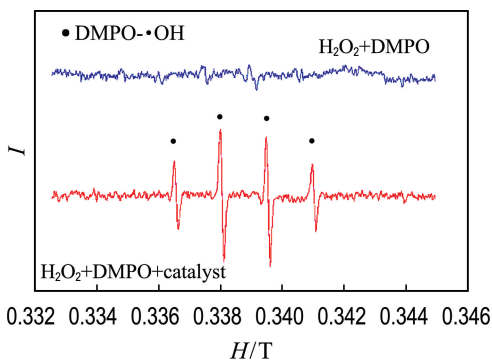
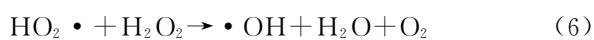
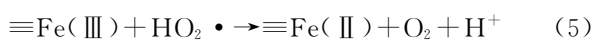
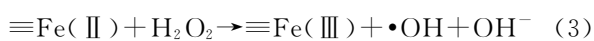


Fig. 14 EPR spectra of  $\text{DMPO}$ -radical adducts in different reaction systems



### 3 Conclusions

In summary, a kind of  $\text{Fe}_2\text{O}_3/\text{Al}_2\text{O}_3$  catalytic membrane for CWPO was prepared by sol-gel method and calcination process on tubular ceramic membranes. The pore size of catalytic membrane is about 50 nm after optimized by 3% PVA and 10 coating times. In the further CWPO experiments, the  $\text{Fe}_2\text{O}_3/\text{Al}_2\text{O}_3$  catalytic membrane exhibits high activity for complete phenol degradation and 70% TOC removal rate within 150 min under 90 °C, 0.4 MPa pressure, pH 6 and 20 mmol/L  $\text{H}_2\text{O}_2$  reaction conditions. Moreover, iron leaching concentration is only 0.41 mg/L and the stability of membrane is good after five consecutive experiments. The main reactive oxidation species in this reaction is  $\cdot\text{OH}$ . This work has a prospect using in practical application and provides some thoughts about the treatment of high concentration organic wastewater with tubular membranes.

### References:

- [1] SUN Dezhi. **Advanced Oxidation Technologies in Environmental Engineering** [M]. Beijing: Chemical Industry Press, 2002. (in Chinese)
- [2] KIM Kyoungun, IHM Sonki. Heterogeneous catalytic wet air oxidation of refractory organic pollutants in industrial wastewaters: a review [J]. **Journal of Hazardous Materials**, 2011, **186**(1): 16-34.
- [3] YAN Ying, JIANG Songshan, ZHANG Huiping, *et al.* Preparation of novel Fe-ZSM-5 zeolite membrane catalysts for catalytic wet peroxide oxidation of phenol in a membrane reactor [J]. **Chemical Engineering Journal**, 2015, **259**: 243-251.
- [4] LIU Y, SUN D. Effect of  $\text{CeO}_2$  doping on catalytic activity of  $\text{Fe}_2\text{O}_3/\text{gamma-Al}_2\text{O}_3$  catalyst for catalytic wet peroxide oxidation of azo dyes [J]. **Journal of Hazardous Materials**, 2007, **143**(1/2): 448-454.
- [5] GAO Han, ZHAO Binxia, LUO Jinchao, *et al.* Fe-Ni-Al pillared montmorillonite as a heterogeneous catalyst for the catalytic wet peroxide oxidation degradation of Orange Acid II: Preparation condition and properties study [J]. **Microporous and**

- Mesoporous Materials**, 2014, **196**: 208-215.
- [6] LIU Yefei, PENG Minghua, JIANG Hong, *et al.* Fabrication of ceramic membrane supported palladium catalyst and its catalytic performance in liquid-phase hydrogenation reaction [J]. **Chemical Engineering Journal**, 2017, **313**: 1556-1566.
- [7] ZHANG Shuo, QUAN Xie, WANG Dong. Catalytic ozonation in arrayed zinc oxide nanotubes as highly efficient mini-column catalyst reactors (MCRs): Augmentation of hydroxyl radical exposure [J]. **Environmental Science and Technology**, 2018, **52**(15): 8701-8711.
- [8] KRIVOSHAPKIN P V, MIKHAYLOV V I, KRIVOSHAPKINA E F, *et al.* Mesoporous Fe-alumina films prepared via sol-gel route [J]. **Microporous and Mesoporous Materials**, 2015, **204**: 276-281.
- [9] DENG Yuheng, CHEN J T, CHANG C H, *et al.* A drying-free, water-based process for fabricating mixed-matrix membranes with outstanding pervaporation performance [J]. **Angewandte Chemie**, 2016, **55**(41): 12793-12796.
- [10] VEDRTNAM A. Fabrication and characterization of cow dung-polyvinyl alcohol composite film [J]. **Composites Communications**, 2018, **8**: 31-35.
- [11] WU Di, HU Zhen, ZHANG Xuqi, *et al.* Remarkable lignin degradation in paper wastewaters over  $\text{Fe}_2\text{O}_3/\gamma\text{-Al}_2\text{O}_3$  catalysts using the catalytic wet peroxide oxidation method [J]. **RSC Advances**, 2017, **7**(60): 37487-37494.
- [12] XU Lejin, WANG Jianlong. A heterogeneous Fenton-like system with nanoparticulate zero-valent iron for removal of 4-chloro-3-methyl phenol [J]. **Journal of Hazardous Materials**, 2011, **186**(1): 256-264.
- [13] INCHAURRONDO N, HAURE P, FONT J. Nanofiltration of partial oxidation products and copper from catalyzed wet peroxidation of phenol [J]. **Desalination**, 2013, **315**: 76-82.
- [14] BACH A, SHEMER H, SEMIAT R. Kinetics of phenol mineralization by Fenton-like oxidation [J]. **Desalination**, 2010, **264**(3): 188-192.
- [15] QUINTANILLA A, FRAILE A F, CASAS J A, *et al.* Phenol oxidation by a sequential CWPO-CWAO treatment with a Fe/AC catalyst [J]. **Journal of Hazardous Materials**, 2007, **146**(3): 582-589.
- [16] CARRIAZO J, GUELOU E, BARRAULT J, *et al.* Catalytic wet peroxide oxidation of phenol by pillared clays containing Al-Ce-Fe [J]. **Water Research**, 2005, **39**(16): 3891-3899.

## 催化湿式过氧化氢氧化耦合 $\text{Fe}_2\text{O}_3/\text{Al}_2\text{O}_3$ 膜分离处理有机废水

刘 玮 玮, 全 燮\*, 陈 硕, 于 洪 涛, 杜 磊

(大连理工大学 工业生态与环境工程教育部重点实验室, 辽宁 大连 116024)

**摘要:** 为提高有机废水的降解效率,设计了一种耦合陶瓷管式膜分离和催化湿式过氧化氢氧化(CWPO)技术的反应器.通过溶胶凝胶法将  $\text{Fe}_2\text{O}_3/\text{Al}_2\text{O}_3$  催化剂涂覆到陶瓷管式膜基底上.并通过控制 PVA 的浓度和涂覆次数,将制备的膜孔径优化到超滤范围.在进行的 CWPO 实验中,优化了 pH、温度、压力和  $\text{H}_2\text{O}_2$  浓度操作条件.实验表明,在 20 mmol/L  $\text{H}_2\text{O}_2$ , pH=6.90 °C 和 0.4 MPa 的反应条件下,苯酚在 150 min 内能完全降解,TOC 去除率为 70%.5 次连续重复实验和溶出测试表明  $\text{Fe}_2\text{O}_3/\text{Al}_2\text{O}_3$  陶瓷膜具有良好的稳定性和可重复性.该反应器耦合 CWPO 与膜分离技术为有机废水处理领域提供了新的思路.

**关键词:** 催化湿式过氧化氢氧化; $\text{Fe}_2\text{O}_3/\text{Al}_2\text{O}_3$  膜催化剂;苯酚;高级氧化技术

**中图分类号:** X703.5

**文献标识码:** A

**doi:** 10.7511/dllgxb201906006

收稿日期: 2019-05-20; 修回日期: 2019-10-10.

基金项目: 国家自然科学基金资助项目(重大项目 21590813);辽宁省兴辽英才计划资助项目(XLYC1801003).

作者简介: 刘玮玮(1994-),女,硕士生,E-mail:2012liuyiwei@mail.dlut.edu.cn;全燮\*(1960-),男,教授,E-mail:quanxie@dlut.edu.cn.